AIP Applied Physics Letters

An electrically switchable surface free energy on a liquid crystal and polymer composite film

Yi-Hsin Lin, Ting-Yu Chu, Yu-Shih Tsou, Kai-Han Chang, and Ya-Ping Chiu

Citation: Applied Physics Letters **101**, 233502 (2012); doi: 10.1063/1.4769093
View online: http://dx.doi.org/10.1063/1.4769093
View Table of Contents: http://scitation.aip.org/content/aip/journal/apl/101/23?ver=pdfcov
Published by the AIP Publishing

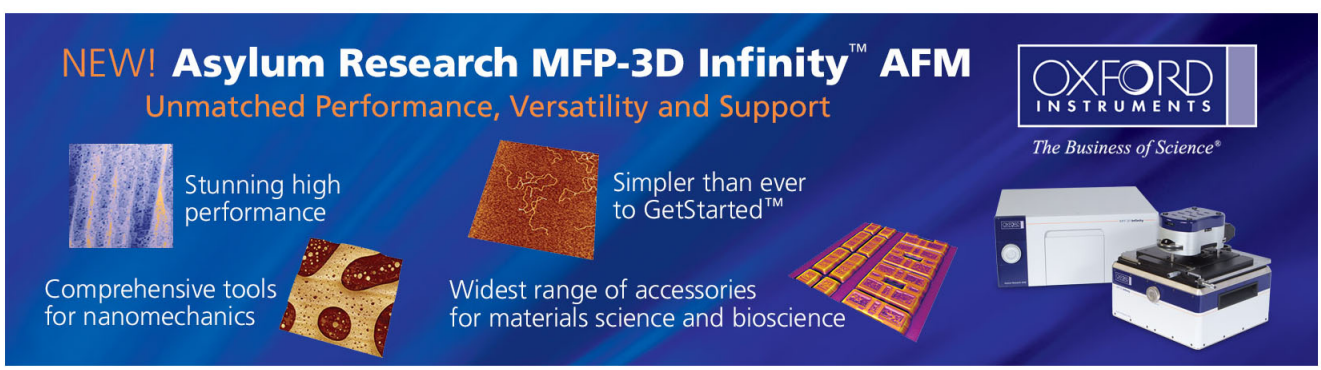

An electrically switchable surface free energy on a liquid crystal and polymer composite film

Yi-Hsin Lin,[1,a)] Ting-Yu Chu,[1] Yu-Shih Tsou,[1] Kai-Han Chang,[1] and Ya-Ping Chiu[2]
[1]*Department of Photonics, National Chiao Tung University, Hsinchu, Taiwan*
[2]*Department of Physics and Center for Nanoscience and Nanotechnology, National Sun Yat-sen University, Kaohsiung 804, Taiwan*

(Received 23 October 2012; accepted 13 November 2012; published online 4 December 2012)

An electrically switchable surface free energy on a liquid crystal and polymer composite film (LCPCF) resulting from the orientations of liquid crystal molecules is investigated. By modification of Cassie's model and the measurement based on the Chibowski's film pressure model (E. Chibowski, Adv. Colloid Interface Sci. **103**, 149 (2003)), the surface free energy of LCPCF is electrically switchable from 36×10^{-3}J/m^2 to 51×10^{-3}J/m^2 while the average tilt angle of LC molecules changes from 0° to 32° with the applied pulsed voltage. The switchable surface free energy of LCPCF can help us to design biosensors and photonics devices, such as electro-optical switches, blood sensors, and sperm testers. © *2012 American Institute of Physics*. [http://dx.doi.org/10.1063/1.4769093]

Electrically switchable surfaces are important in photonics devices and biosensors. The main mechanism of switchable surfaces is based on switchable wettability resulting from molecular conformations under external stimuli by adopting delicate crafts of self-assembly-monolayer.[1,2] Recently, we have developed a switchable surface, liquid crystal and polymer composite film (LCPCF), and also versatile promising applications based on LCPCF, such as electrically tunable focusing lenses, polarizer-free electro-optical switches, sperm testing devices, and biosensors.[3–8] From many qualitatively macroscopically experimental observation and the measurement of the attractive force between the tip of an atomic force microscopy (AFM) and LCPCF surface, the switchable wetting properties of LCPCF seems to result from orientations of liquid crystal molecules anchored among the polymer grains under applied pulsed voltages.[3,9,10] However, the relationship between orientations of liquid crystal molecules and the electrically tunable surface free energy (or surface tension) of LCPCF is still unclear and needs to be investigated. In this paper, we experimentally investigate the relationship between orientations of liquid crystal molecules and the electrically tunable surface free energy (or surface tension) of LCPCF. According to the modified Cassie's model and the measurement based on the Chibowski's film pressure model, the surface free energy of LCPCF is electrically switchable from 36×10^{-3}J/m^2 to 51×10^{-3}J/m^2 while the average tilt angle of LC molecules changes from 0° to 32°. The switchable range of surface free energy of LCPCF affects the performance of different biosensors and photonics devices, such as electro-optical switches, blood sensors, and sperm testers. This study helps us to understand the mechanism of the switchable surface of LCPCF and then further assists designing biosensors and photonics devices.

The structure of LCPCF is illustrated in Fig. 1. The structure consists of a LCPCF on a patterned indium tin oxide (ITO) glass substrate, which provides fringing electric fields to LCPCF. The ITO electrodes on the glass substrate were etched with interdigitated chevron patterns, shown as the zigzag electrodes. The zigzag ITO strips have corner angles of 150°. The width and the gap of the electrode strips are 4 and 14 μm, respectively. The magnification of the interface between the fluidic droplet and the LCPCF surface is exaggeratedly shown in the inlet in Fig. 1. In the inlet, the surface of the LCPCF consists of polymer grains and liquid crystals anchored among the polymer grains. The liquid crystals are aligned along x-direction at voltage-off state. At the voltage-on state, the liquid crystal molecules are re-orientated by the fringing electric fields, and then the surface is more hydrophilic.[3] To fabricate LCPCF on the ITO glass substrate, we mixed a nematic LC mixture E7 (Merck) and a liquid crystalline monomer (4-(3-acryloyloxypropyloxy)-benzoic acid 2-methyl-1, 4-phenylene ester) at 70:30 wt. % ratios. The nematic LC (E7) consists of four compounds: 5CB (4-pentyl-4′-cyanobiphenyl), 7CB (4-heptyl-4′-cyanobiphenyl), 8OCB (4-octyloxy-4′-cyanobiphenyl), and 5CT (4-pentyl-4′-cyanoterphenyl). The detail chemical structures of E7 are also

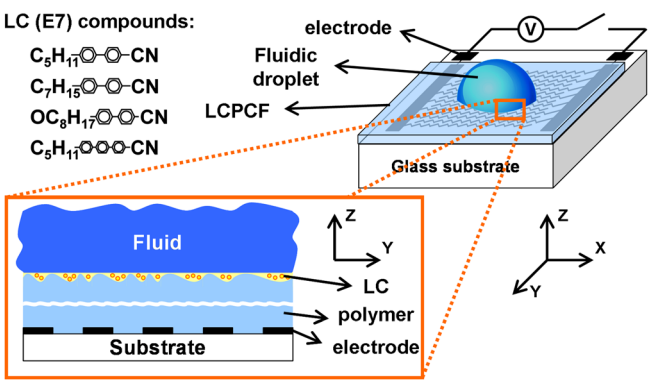

FIG. 1. The LCPCF on a glass substrate with patterned electrodes and the magnification of the interface between the fluidic droplet and the LCPCF surface is exaggeratedly in the inlet. The chemical structures of LC(E7) compounds are listed as well.

[a)]Author to whom correspondence should be addressed. Electronic mail: yilin@mail.nctu.edu.tw.

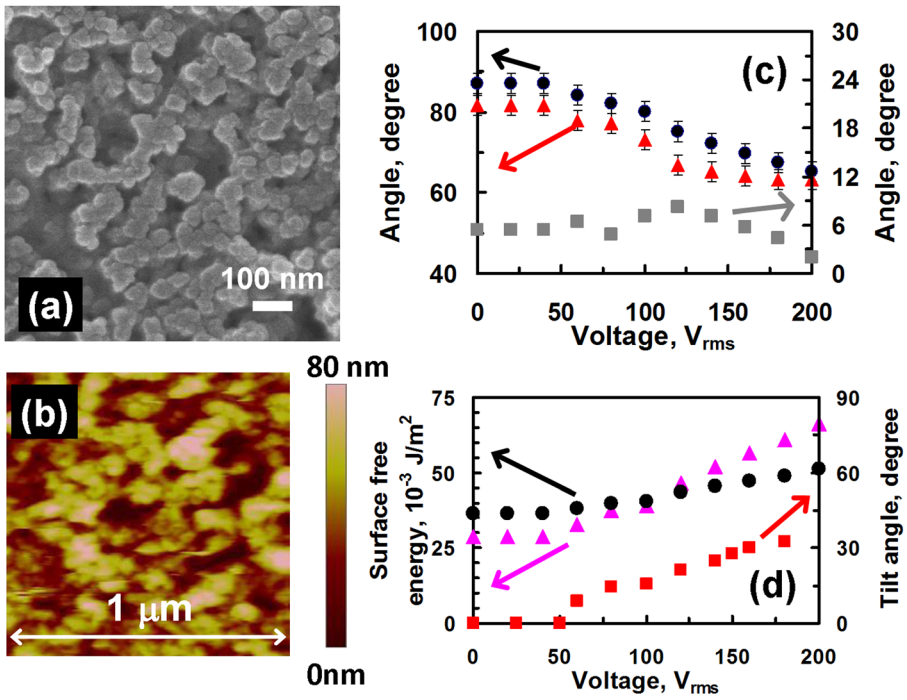

FIG. 2. (a) SEM image and (b) AFM image of LCPCF. (c) The voltage-dependent advancing angle (black dots), the voltage-dependent receding angle (red triangles), and the voltage-dependent hysteresis (gray squares) of the LCPCF. ($T_{curing} = 70\,^{\circ}C$). (d) The surface free energy as a function of voltage of LCPCF (black dots) and LC molecules (pink triangles). The average tilt angle of LC molecules as a function of voltage is also shown (red squares).

drawn in Fig. 1. The mixtures were then filled into an empty cell with a gap of $\sim 7\,\mu m$, which consists of a top glass substrate and a patterned ITO glass substrate (bottom substrate). The top glass substrate of the cell was coated with a thin polyimide (PI) layer and then mechanically buffed along x-axis. After we filled the mixture into the cell, the cell was then exposed to a UV light with intensity $I = 10$ mW/cm^2 for $\sim$60 min at a curing temperature of 70 °C (or $T_{curing} = 70\,^{\circ}C$). After the phase separation and the photo-polymerization process, the top glass substrate was peeled off with a thermal-releasing process. A solidified LCPCF was then obtained. Fig. 2(a) shows the SEM (scanning electron microscopy) image of LCPCF after we removed LC using hexane, and Fig. 2(b) shows the AFM image of LCPCF using the tapping mode of AFM. In Figs. 2(a) and 2(b), the surface of LCPCF indeed is made up of polymer grains and LC anchored among the polymer grains. The average polymer grain size is $\sim$70 nm, and the average domain size is $\sim$225 nm.

Generally speaking, a surface free energy (or surface tension) of a smooth solid surface in the vapor can be determined by dropping a fluidic droplet on the solid surface and the surface free energy is described according to the Young's contact angle, which is a result of a balance of three phases: vapor, liquid, and solid. The surface free energy is modified by the roughness according to the Wenzel's magnification of wettability. When the solid surface is made up of several materials or so-called chemical heterogeneity, the surface free energy can be further re-modified according to the Cassie's linear composition of interfacial energies of several wetting materials. The Young's balance of three phases, Wenzel's magnification of wettability and Cassie's chemical heterogeneity are the factors that can help us to describe the wetting properties or surface free energy of a surface.[11] However, one more factor, molecular orientations, should be considered in order to fully describe the mechanism of the switchable wettability on LCPCF.

In order to quantitatively investigate the relation between the orientations of LC molecules and surface free energy of LCPCF, we first measure the surface free energy of LCPCF by measuring the hysteresis of the LCPCF. The hysteresis of the LCPCF is defined as the difference between an advancing angle (θ_a) and a receding angle (θ_r) of a fluidic drop (de-ionized water drop) on the LCPCF. The advancing angle (θ_a) and the receding angle (θ_r) are the angles at which the contact line changes when the volume of the fluidic drop increases and decreases, respectively. To measure θ_a and θ_r, we increased and decreased the volume of the fluidic drop on LCPCF, then recorded the image of the fluidic drop at which the contact line changed by a CCD camera (JAI CV-M30) with a frame rate of 120 frames/s, and measured the contact angles with a system of contact angle measurement (FTA 1000 Analyzer System). The measured advancing angle (black dots), the measured receding angle (red triangles), and the hysteresis (gray squares) of the LCPCF as a function of the applied pulsed voltage (V) are shown in Fig. 2(c). The advancing angle and the receding angle decrease with an increase of the applied pulsed voltage when V is larger than the threshold voltage ($V_{th} \sim 50$ V_{rms}). The hysteresis of LCPCF increases first as $V_{th} < V < 125$ V_{rms} and then decreases as $V > 125$ V_{rms}. According to the Chibowski's film pressure model, the surface free energy of the LCPCF in the air ($\gamma_{LCPCF\text{-}air}$) with an unit of J/m^2 can be expresses as[12]

$$\gamma_{LCPCF-air}(\phi(V)) = \frac{\gamma_{L-air} \times (1 + \cos\theta_a(V))^2}{2 + \cos\theta_r(V) + \cos\theta_a(V)}, \qquad (1)$$

where $\gamma_{L\text{-}air}$ is the surface free energy of the testing fluid in the air, and ϕ is the average tilt angle of LC molecules with respect to x-axis in Fig. 1. As a result, the surface free energy of the LCPCF can be calculated and shown in black dots in Fig. 2(d). The surface free energy of the LCPCF increases from 36×10^{-3}J/m^2 to 51×10^{-3}J/m^2 with the applied

pulsed voltage. According to Cassie's model, the surface free energy of LCPCF in the air is a linear composition of the surface free energies of polymer ($\gamma_{\text{p-air}}$) and the surface free energy of LC ($\gamma_{\text{LC-air}}$)

$$\gamma_{LCPCF-air}(\phi(V)) = R_w \times [f_{LC} \times \gamma_{LC-air}(V) + f_p \times \gamma_{p-air}], \tag{2}$$

where R_w is the roughness factor defined as the ratio of the actual surface area to the geometric surface area, f_{LC} is the fraction of LC, and f_p is the fraction of polymer. From Eqs. (1) and (2), the surface free energy of LC ($\gamma_{\text{LC-air}}$) can thus be expressed in Eq. (3)

$$\gamma_{LC-air}(\phi(V)) = \frac{1}{R_w \times f_{LC}} \times \left[\gamma_{L-air} \times \frac{(1+\cos\theta_a(V))^2}{2+\cos\theta_r(V)+\cos\theta_a(V)} - R_w \times f_p \times \gamma_{p-air}\right]. \tag{3}$$

From SEM image and AFM image in Figs. 2(a) and 2(b), the LC domain can be estimated as ~225 nm and the root-mean-square (RMS) roughness is ~15 nm. Based on the cubic approximation of LC domain, R_w is then can be calculated as 1.214. By using a software: IMAGEJ (National Institutes of Health) to analyze the SEM and AFM images, f_{LC} and f_p are 0.32 and 0.68, respectively. $\gamma_{\text{p-air}}$ is around ~30.9 J/m^2 obtained by putting the measured θ_a and θ_r of pure polymeric film without LC into Eq. (1). The testing fluid is de-ionized water in the experiment and then $\gamma_{\text{L-air}} \sim 72.8 \times 10^{-3}$J/m^2. From the data in Fig. 2(c), related measured parameters, and Eq. (3), we could plot $\gamma_{\text{LC-air}}$ as a function of the applied pulsed voltage as shown in pink triangles in Fig. 2(d). At V = 0, the surface free energy of the LC molecules is 29×10^{-3}J/m^2, which is also the surface free energy of phenyl/terphenyl part of LC materials because the LC molecules were arranged to align along x direction (in Fig. 1). The direction of the alignment was experimentally confirmed in Ref. 6. In Fig. 2(d), the surface free energy of the LC molecules increases from 29×10^{-3}J/m^2 to 66×10^{-3}J/m^2 with the applied pulsed voltage. The increase of surface free energy of LCPCF results from the increase of surface free energy of LC molecules under applied pulsed voltages. Moreover, the LC molecules tilt up when $V > V_{th}$. However, we still do not know the average tilt angle of LC molecules.

In order to further calculate the average tilt angle of LC molecules, we have to know the anisotropic surface free energy of LC molecules. The LC materials of LCPCF consisting of 4 compounds can simply be divided by three parts: the alkyl/alkoxy chain, the cyano (CN) group, and the phenyl/terphenyl part. We then define $\gamma_{\text{ph-ter}}$, $\gamma_{\text{alky-alko}}$, and γ_{CN} as the surface free energy of phenyl/terphenyl part, alkyl chain, and cyano group, respectively. $\gamma_{\text{ph-ter}}$ was obtained ~29×10^{-3}J/m^2 in Fig. 2(d) and $\gamma_{\text{alky-alko}} \sim \gamma_{\text{alkyl}} \sim 29 \times 10^{-3}$J/m^2.[13] However, γ_{CN} is still unknown. To estimate γ_{CN}, we performed an experiment, as shown in Fig. 3(a). We dropped a de-ionized water droplet (~1 μl) on a thin layer of nematic LC with a single compound 5CB (4-Cyano-4′-pentylbiphenyl), which was on the top of a vertical alignment

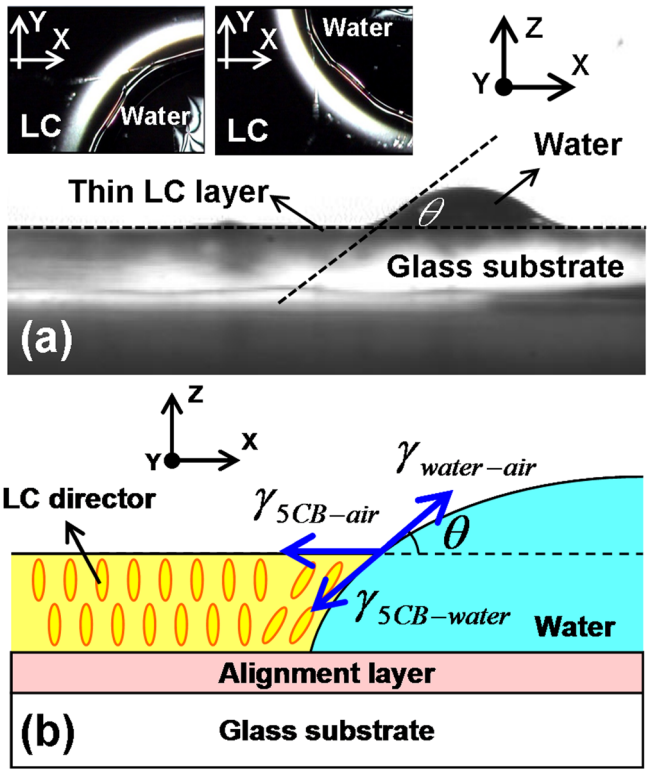

FIG. 3. (a) The experiment of measuring the surface free energy of 5CB. A water droplet was dropped on a thin layer of LC (5CB). The inlets are the top views of the water droplet and the droplet is rotated 90° under crossed polarizers. The transmissive axes of polarizer and analyzer are parallel to x-axis and y-axis, respectively. (b) The detail illustration of (a).

layer, as depicted in Fig. 3(b). The water droplet sank into the LC layer and touched the vertical alignment layer. We observed the area near the droplet under crossed polarizers and also rotated the glass substrate, as shown in the inlet of Fig. 3(a). The LC region remains dark under the rotation. That means the LC molecules are perpendicular to the LC-air interface. The liquid crystal molecules are vertically aligned because of three reasons: thin LC layer, the anchoring force of the bottom alignment layer, and the anchoring force from the inclination of homeotropic alignment at the LC-air interface.[14] At the interface among air, water, and liquid crystals in Fig. 3(b), three phases were balanced by following Young's equation: $\gamma_{water-air} = \gamma_{5CB-air} \times \cos\theta + \gamma_{5CB-water}$, where θ is contact angle in Fig. 3(b). $\gamma_{\text{water-air}}$, $\gamma_{\text{5CB-air}}$, and $\gamma_{\text{5CB-water}}$ represents the surface free energies between water and air, between LC and air, and between LC and de-ionized water, respectively. The $\gamma_{\text{5CB-air}}$ is then calculated ~57.97×10^{-3}J/m^2 after putting the parameters in the experiment: the measured $\theta \sim 36.17°$, $\gamma_{\text{water-air}} \sim 72.8 \times 10^{-3}$J/m^2, and $\gamma_{\text{5CB-water}} \sim 26 \times 10^{-3}$J/m^2.[13] Consider the anisotropic surface free energy and the average tilt angle (ϕ') of LC molecules with respect to x-axis in Fig. 3(b), the surface free energy of 5CB in the air can then be expressed as[14]

$$\gamma_{5CB-air}(\phi'(V)) = \gamma_{\perp-air} \times \sin^2\phi'(V) + \gamma_{//-air} \times \cos^2\phi'(V), \tag{4}$$

where $\gamma_{\perp-air}$ and $\gamma_{//-air}$ are the surface free energies when the LC molecules are perpendicular to the air-LC interface and when the LC molecules are parallel to the air-LC

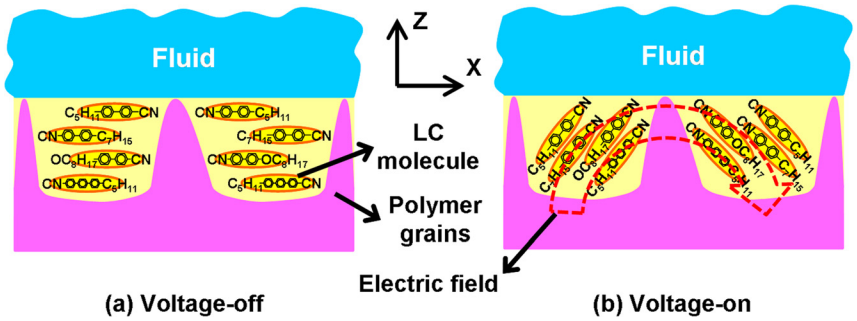

FIG. 4. (a) At voltage-off state, the LC molecules are anchored among the polymer grains. (b) At voltage-on state, the LC molecules are reoriented by the electric field and the cyano groups of LC materials tilt toward the interface between the fluid and LC materials.

interface, respectively. For 5CB in the air, $\gamma_{//-air} = \gamma_{\text{phenyl}} \sim 40 \times 10^{-3}\text{J/m}^2$,[13] and $\phi' = \theta \sim 36.17°$. As a *result*, $\gamma_{\perp-air}$ is calculated as $\sim 91.59 \times 10^{-3}\text{J/m}^2$. In fact, $\gamma_{\perp-air}$ is the linear combination of γ_{CN} and γ_{alkyl} because the arrangement of half of CN-group of 5CB and half of alkyl group of 5CB result in minimum free energy at the air-LC interface.[15] This also means $\gamma_{\perp-air}$ should satisfy the relation: $\gamma_{\perp-air} = 0.5 \times \gamma_{CN} + 0.5 \times \gamma_{alkyl}$. Therefore, γ_{CN} is $\sim 154 \times 10^{-3}\text{J/m}^2$ after calculation.

Next, we calculate the average tilt angle of LC molecules of LCPCF. On LCPCF, the LC molecules anchored among the polymer grains are aligned along x-axis at $V = 0$, and the LC molecules are reoriented with the applied pulsed voltage at $V \gg V_{\text{th}}$. The tilting part of LC molecules should be the CN group (or the polar group) because the de-ionized water we used has strong polar-polar interaction with the CN group of LC materials. As a result, the surface free energy of the LCs anchored among the polymer grains on LCPCF can be expressed as[14] $\gamma_{LC-air}(\phi(V)) = \gamma_{CN} \times \sin^2\phi(V) + \gamma_{ph-ter} \times \cos^2\phi(V)$, where ϕ is the average tilt angle of LC molecules on LCPCF with respect to x-axis. Since $\gamma_{\text{ph-ter}}$ and γ_{CN} are known and $\gamma_{\text{LC-air}}$ is also obtained in Fig. 2(d), we then obtain ϕ as a function of the applied pulsed voltage, as shown in red squares in Fig. 2(d). The LC molecules tilt up from 0° to 32° with the applied pulsed voltage.

From the experiment and analysis above, the detail mechanism of the surface of LCPCF can then be depicted in Figs. 4(a) and 4(b). At voltage-off state, the strong anchoring force which is provided by polymer grains results in the LC molecules aligned along x-direction. The surface free energy of LCPCF results from the interaction between phenyl/terphenyl part of LC (E7) and the testing water, as depicted in Fig. 4(a). When the applied pulsed voltage overcomes the anchoring force of the polymer grains and elastic properties of LC materials, the LC molecules change the orientations gradually. The CN-group tilts up with the applied pulsed voltage because of (1) the fringing electric field, and (2) the strong interaction between polar CN-group and polar fluid (de-ionized water). The CN groups of the LC molecules tilt up with the applied pulsed voltage and the maximum tilt angle is around 32° with respect to x-axis, as illustrated in Fig. 4(b). The surface free energy of LCPCF could be up to $85 \times 10^{-3}\text{J/m}^2$ if the average tilt angle of LC molecules is 90°.

In conclusion, the LC molecular orientation is indeed a factor affecting the surface free energy of LCPCF surface. The molecular orientation re-modifies the conventional Cassie's model for understanding the surface wettability. We can perform the experimental analysis to estimate the orientation-induced change of surface free energy of LCPCF. Moreover, the analysis here can assist us to design LCPCF with various surface free energies in terms of adjusting polarity of LC molecules, fractions of LC materials, roughness of LCPCF, and the distribution of electric fields. Many practical applications based on LCPCF require proper surface free energies. Based on this study, the tunable range of the surface free energy of LCPCF can be manipulated and it is important in biosensors and photonics devices. For example, large tunable focusing range of liquid lenses using LCPCF needs large tunable range of surface free energy.[3] For the electro-optical switches, the response time can be faster with the large change of surface free energy of LCPCF.[6] For the sperm tester, the sensitivity can be even enlarged.[8] In addition, the change of surface free energy of human blood can indicate many human diseases, such as atherogenesis and hyperthyroidism.[16,17] The wetting properties of LCPCF can be designed in a proper range to sense the change of surface free energy of human blood. Furthermore, our LCPCF and the analysis method in this Letter can help us to measure the anisotropic surface free energy of different chemical structure of LC materials.

The authors are indebted to Jun-Lin Chen and Wei-Lin Chu for technical assistance. We appreciate Chimei Optoelectronics for providing ITO glass substrates. This research was supported by National Science Council (NSC) in Taiwan under the Contract No. 101-2112-M-009-011-MY3.

[1]M. K. Chaudhury and G. M. Whitesides, Science **256**, 1539 (1992).
[2]S. L. Gras, T. Mahmud, G. Rosengarten, A. Mitchell, and K. Kalantar-zadeh, Chem. Phys. Chem. **8**, 2036 (2007).
[3]Y. H. Lin, H. Ren, Y. H. Wu, S. T. Wu, Y. Zhao, J. Fang, and H. C. Lin, Opt. Express **16**, 17591 (2008).
[4]Y. H. Lin, H. Ren, Y. H. Wu, Y. Zhao, J. Fang, Z. Ge, and S. T. Wu, Opt. Express **13**, 8746 (2005).
[5]Y. H. Lin, H. Ren, S. Gauza, Y. H. Wu, Y. Zhao, J. Fang, and S. T. Wu, J. Disp. Technol. **2**, 21–25 (2006).
[6]Y. H. Lin, J. K. Li, T. Y. Chu, and H. K. Hsu, Opt. Express **18**, 10104 (2010).
[7]H. C. Lin and Y. H. Lin, Appl. Phys. Lett. **98**, 083503 (2011).
[8]Y. H. Lin, T. Y. Chu, W. L. Chu, Y. S. Tsou, Y. P. Chiu, F. Lu, W. C. Tsai, and S. T. Wu, J. Nanomedicine Nanotechnol. **S9**, 001 (2011).
[9]Y. P. Chiu, C. Y. Shen, and Y. H. Lin, Jpn. J. Appl. Phys., Part 1 **49**, 071604 (2010).
[10]Y. P. Chiu, C. Y. Shen, W. C. Wang, T. Y. Chu, and Y. H. Lin, Appl. Phys. Lett. **96**, 131902 (2010).
[11]P. De Gennes, F. Brochard-Wyart, and D. Quere, *Capillarity and Wetting Phenomena Drops, Bubbles, Pearls, Waves* (Springer-Verlag, Berlin, 2004).
[12]E. Chibowski, Adv. Colloid Interface Sci. **103**, 149 (2003).
[13]U. Delabre, C. Richard, and A. M. Cazabat, J. Phys.: Condens. Matter **1**, 464129 (2009).
[14]A. A. Sonin, *The Surface Physics of Liquid Crystals* (Gordan and Breach, 1995).
[15]I. Cacelli, L. D. Gaetani, G. Prampolini, and A. Tani, Mol. Cryst. Liq. Cryst. **465**, 175 (2007).
[16]P. D. Somer, J. V. D. Bosch, and J. V. Joosens, Nature **182**, 59 (1958).
[17]E. G. Nicholls and G. A. Harrop, Jr., J. Clin. Invest. **5**, 181 (1928).